

CoE4TN4

Image Processing

Chapter 5

Image Restoration and  
Reconstruction



---

# Image Restoration

- Similar to image enhancement, the ultimate goal of restoration techniques is to improve an image
- Restoration: a process that attempts to reconstruct or recover a degraded image by using some a priori knowledge of the degradation phenomenon.
- Technique: model the degradation -> apply the inverse process to recover the original image
- Enhancement technique are heuristic while restoration techniques are mathematical

# Degradation Model

- Problem: given  $g(x,y)$  and  $H$  find an approximate of  $f(x,y)$ .
- Some statistical knowledge of  $n(x,y)$  is available.

$$g(x,y) = h(x,y) * f(x,y) + n(x,y)$$

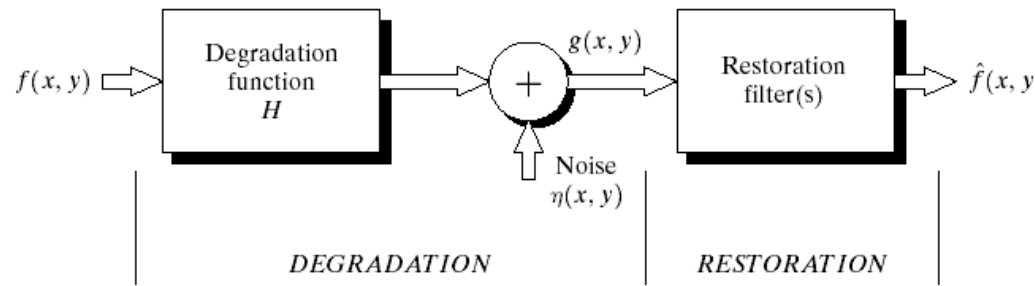
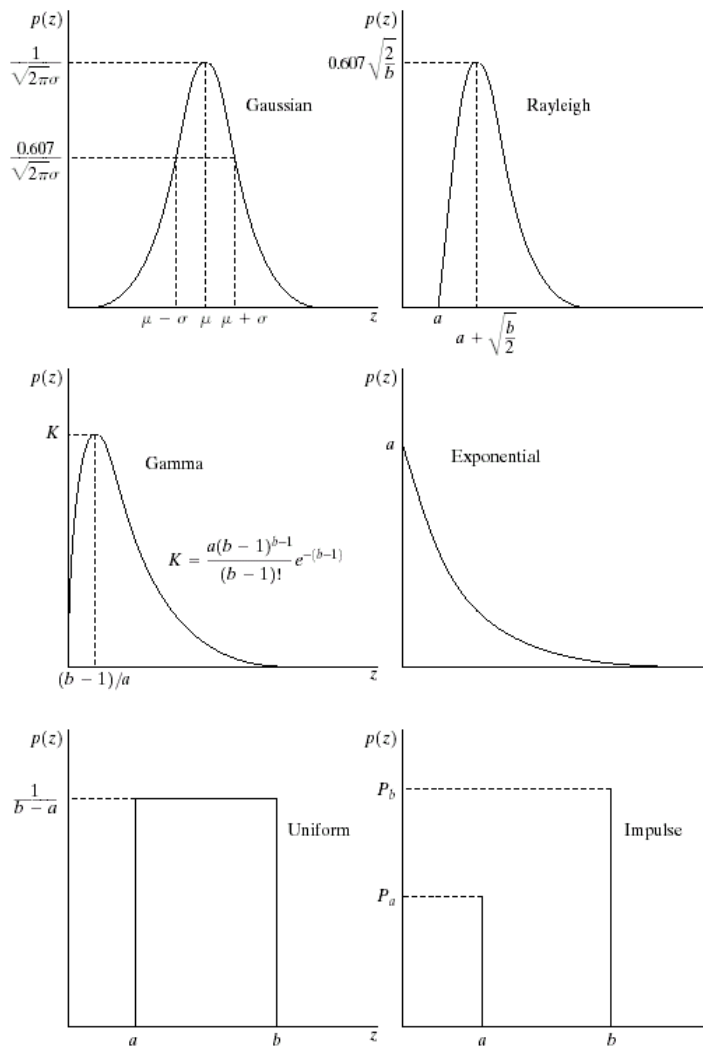


**FIGURE 5.1** A model of the image degradation/ restoration process.

---

# Noise model

- Principal sources of noise in digital images: during image acquisition, during image transmission
- Image acquisition: image sensor might produce noise because of environmental conditions or quality of sensing elements
- Image transmission: interference in the channel
- Assumptions: noise is independent of spatial coordinates (except for periodic noise) and independent of the image
- Spatial description of noise: statistical behavior of the values of the noise (PDF)
- Most common PDFs found in image processing: Gaussian noise, Rayleigh noise, Erlang (Gamma) noise, Exponential noise, Uniform noise, Impulse noise



---

# Noise model

- Different PDFs provide useful tools for modeling a broad range of noise corruption situations:
- Gaussian noise: due to factors such as electronic circuit noise, sensor noise (due to poor illumination or high temperature)
- Rayleigh noise: model noise in range imaging
- Exponential and Gamma: laser imaging
- Impulse noise: found in quick transients (e.g., faulty switches)

---

# Noise model

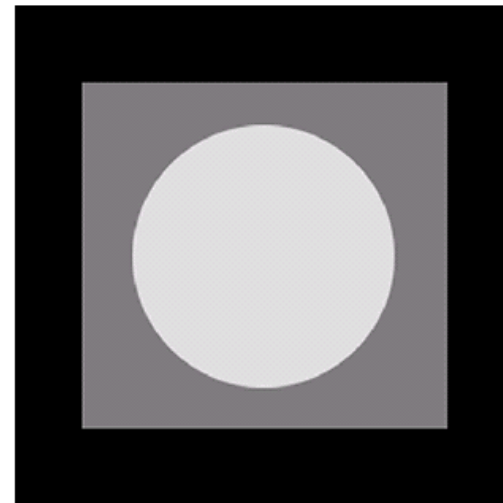


**FIGURE 5.3** Test pattern used to illustrate the characteristics of the noise PDFs shown in Fig. 5.2.

---

# Noise model

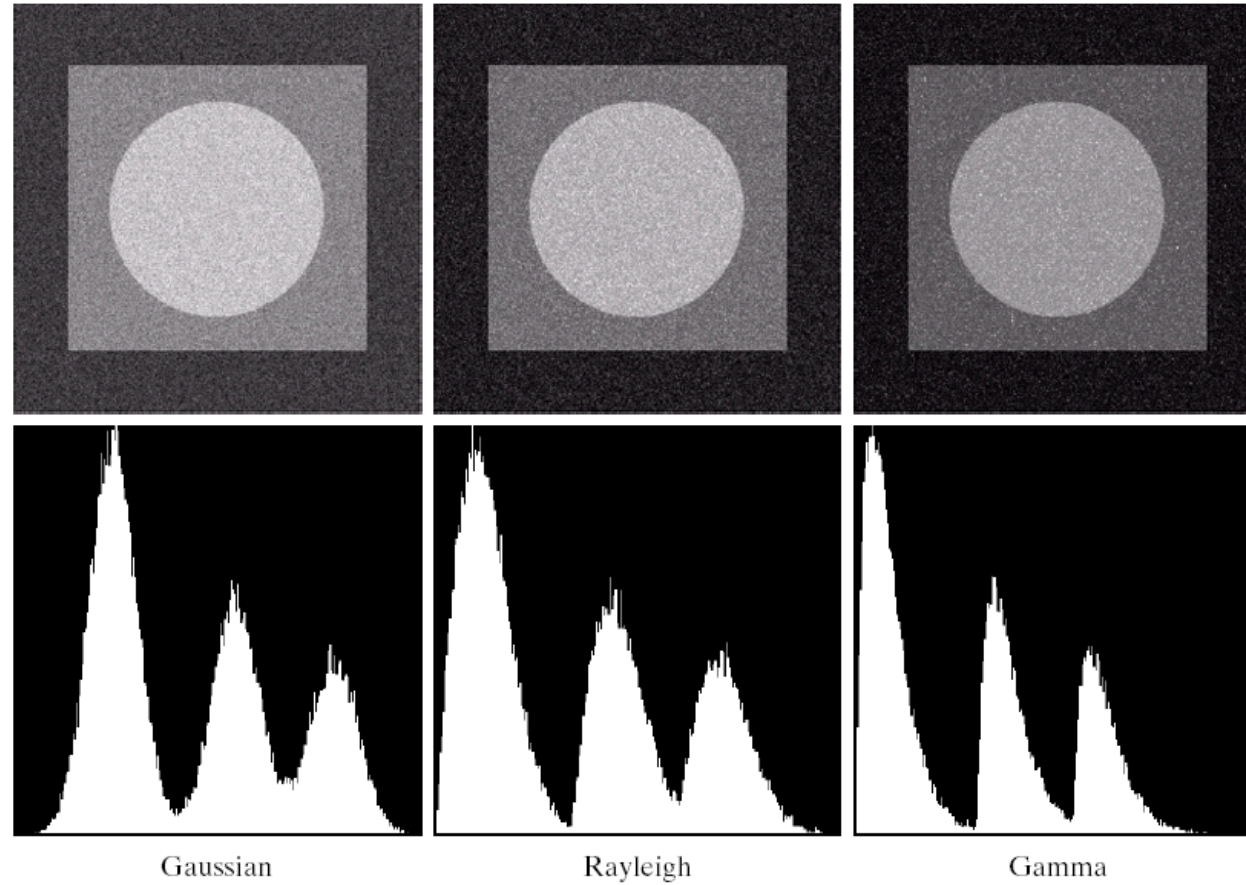
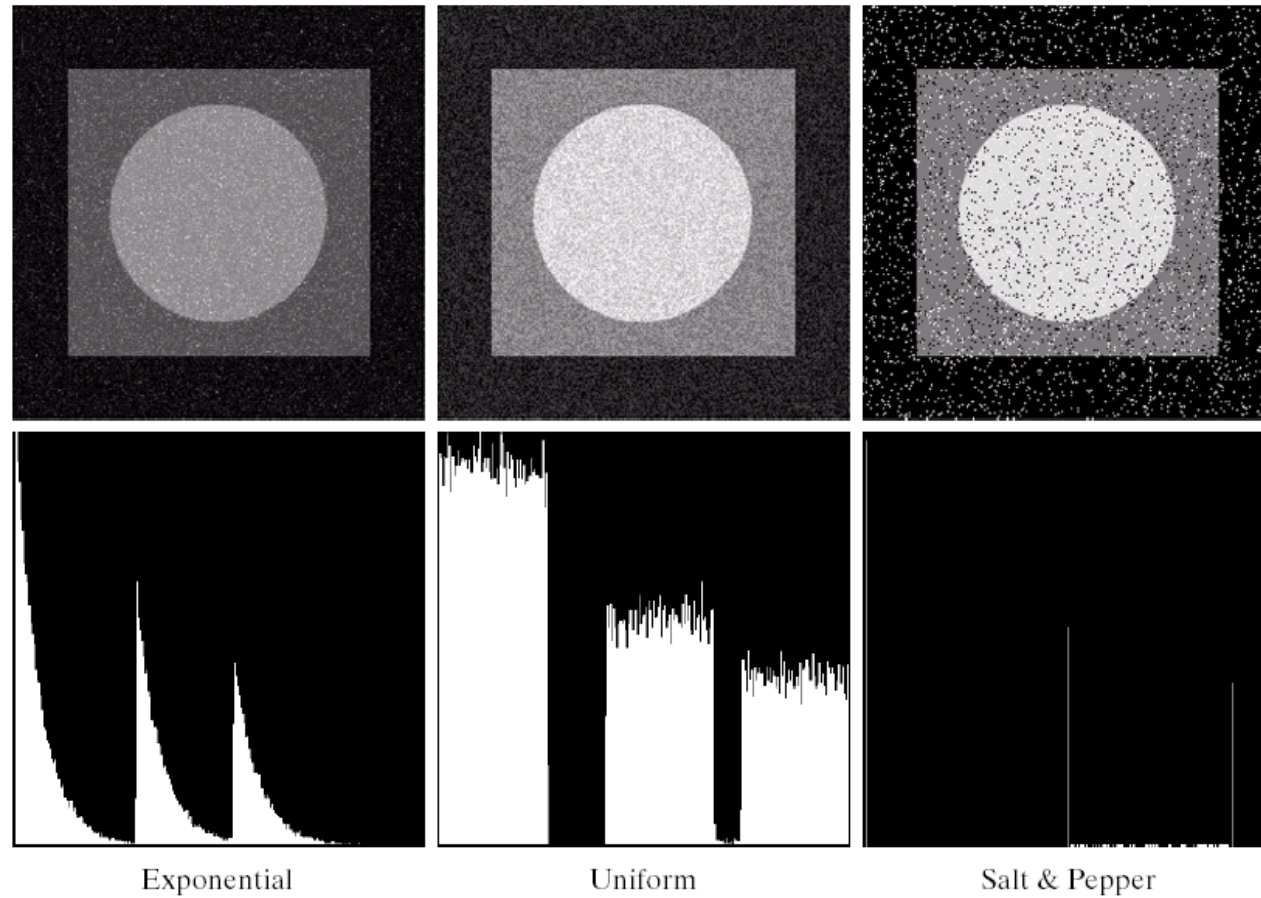


**FIGURE 5.4** Images and histograms resulting from adding Gaussian, Rayleigh, and gamma noise to the image in Fig. 5.3.

# Noise model



g h i

j k l

**FIGURE 5.4 (Continued)** Images and histograms resulting from adding exponential, uniform, and impulse noise to the image in Fig. 5.3.

---

# Periodic Noise

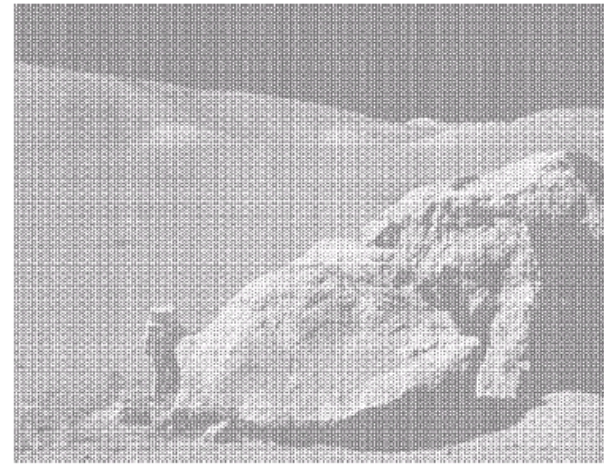
- Periodic noise: from electrical or electromechanical interference during image acquisition
- Frequency domain filtering can be used to remove this noise
- Fourier transform of a pure sinusoid is a pair of conjugate impulses
- In the Fourier transform of an image corrupted with periodic noise should have a pair of impulses for each sine wave

# Noise model

a  
b

**FIGURE 5.5**

(a) Image corrupted by sinusoidal noise.  
(b) Spectrum (each pair of conjugate impulses corresponds to one sine wave).  
(Original image courtesy of NASA.)



---

# Noise model

- Parameters of periodic noise are typically estimated by inspection of the FT of the image
- Estimation of parameters of the PDF of noise:
  - If the imaging system is available, one simple way is to capture a set of images of “flat” environments
    - Flat environments: a solid gray board illuminated uniformly
  - If only the images are available, the parameters of the PDF can be estimated from small patches of reasonably constant gray levels

# Noise model

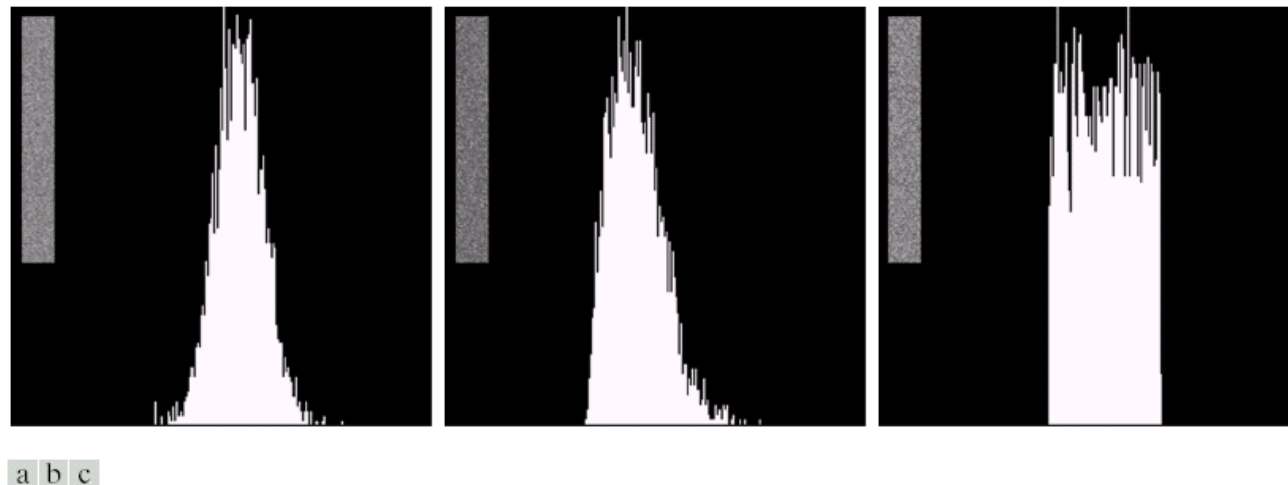


**FIGURE 5.6** Histograms computed using small strips (shown as inserts) from (a) the Gaussian, (b) the Rayleigh, and (c) the uniform noisy images in Fig. 5.4.

---

# Restoration in the presence of noise

- When the only degradation is noise:  
$$g(x,y) = f(x,y) + n(x,y)$$
  
$$G(u,v) = F(u,v) + N(u,v)$$
- Spatial filtering is the method of choice in this case: Mean filters, Order-statistics filters, Adaptive filters

# Mean filters

- $S_{xy}$  set of coordinates in a subimage of size  $m \times n$
- Arithmetic mean filter:

$$\hat{f}(x, y) = \frac{1}{mn} \sum_{(s,t) \in S_{xy}} g(s, t)$$

- Smoothes local variations (noise is reduced because of blurring)
- Geometric mean filter:

$$\hat{f}(x, y) = \left[ \prod_{(s,t) \in S_{xy}} g(s, t) \right]^{\frac{1}{mn}}$$

- Achieves smoothing comparable to arithmetic mean, but tends to lose less image details

# Mean filters

- Harmonic mean filter:

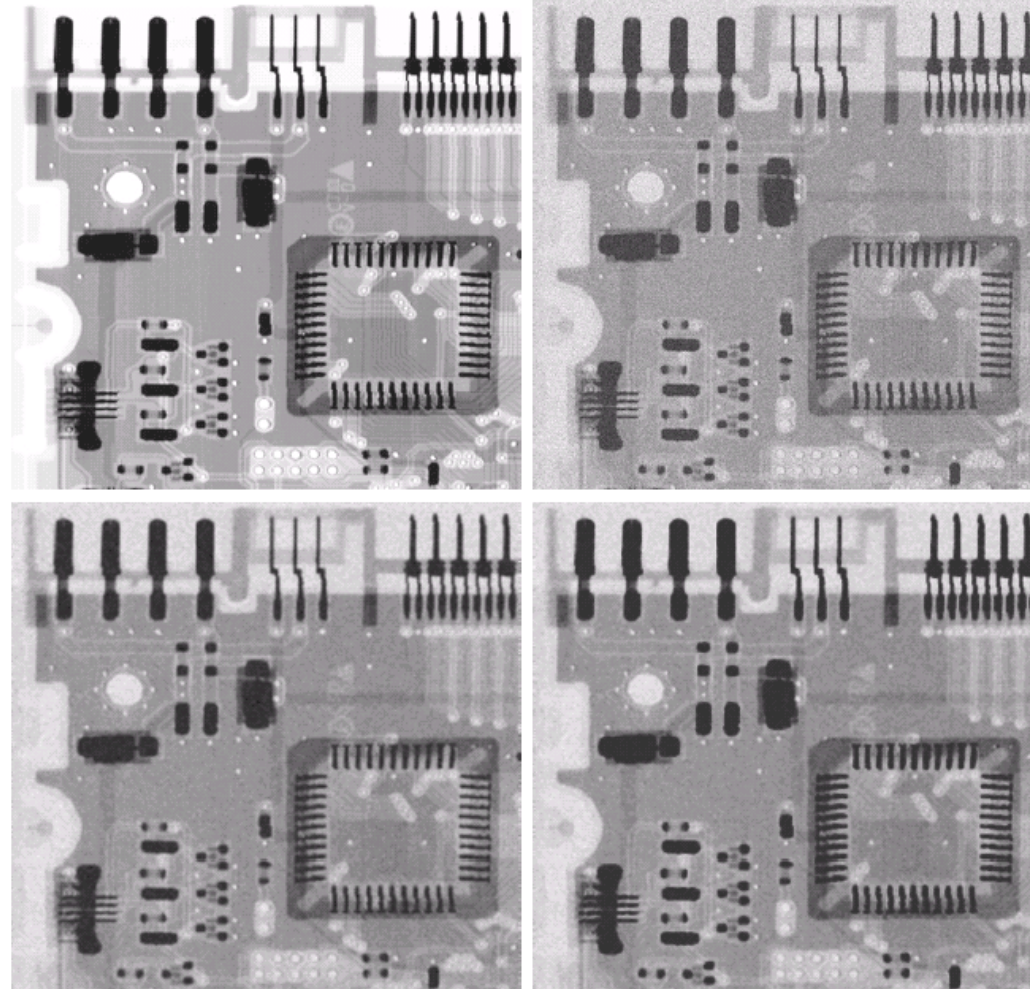
$$\hat{f}(x, y) = \frac{mn}{\sum_{(s,t) \in S_{xy}} \frac{1}{g(s, t)}}$$

- Suitable for salt noise, does well with Gaussian noise

- Contraharmonic mean filter

$$\hat{f}(x, y) = \frac{\sum_{(s,t) \in S_{xy}} g(s, t)^{Q+1}}{\sum_{(s,t) \in S_{xy}} g(s, t)^Q}$$

- Negative Q: Suitable for salt noise
- Positive Q: Suitable for pepper noise



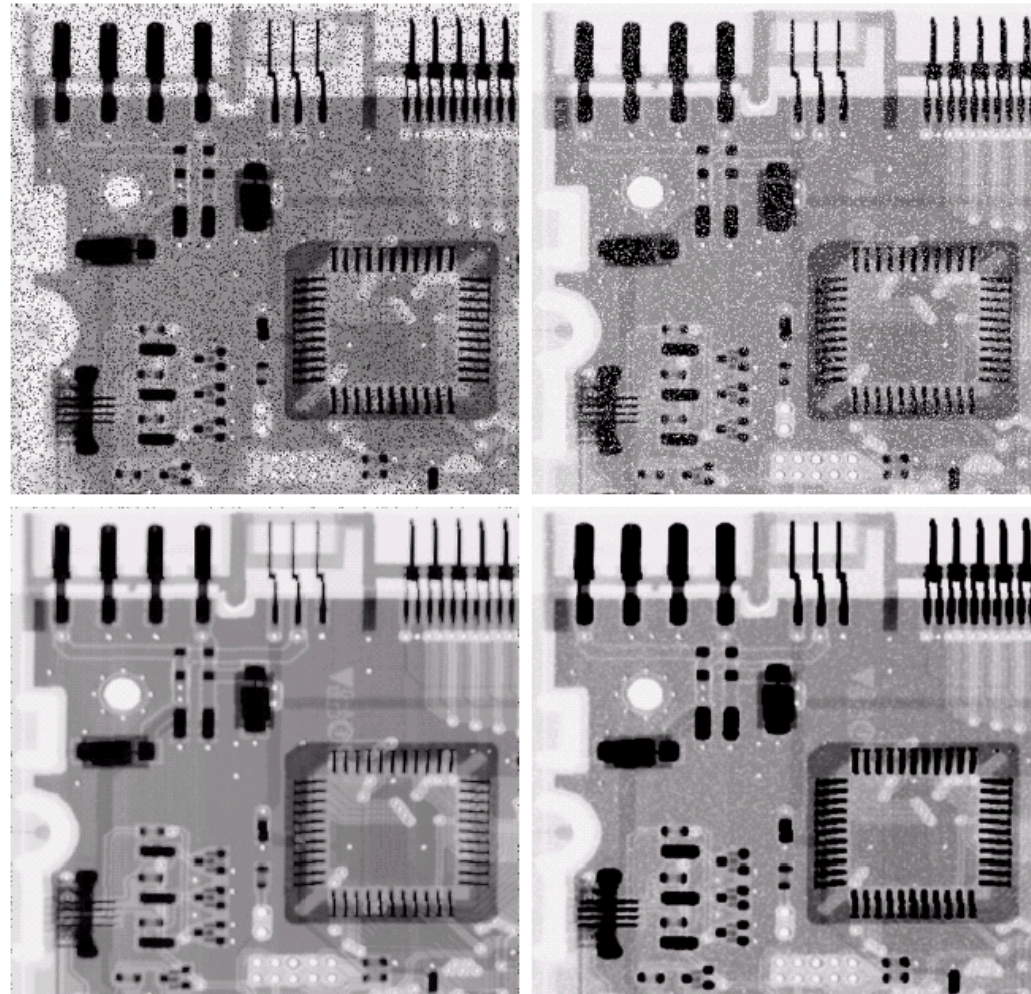
a b  
c d

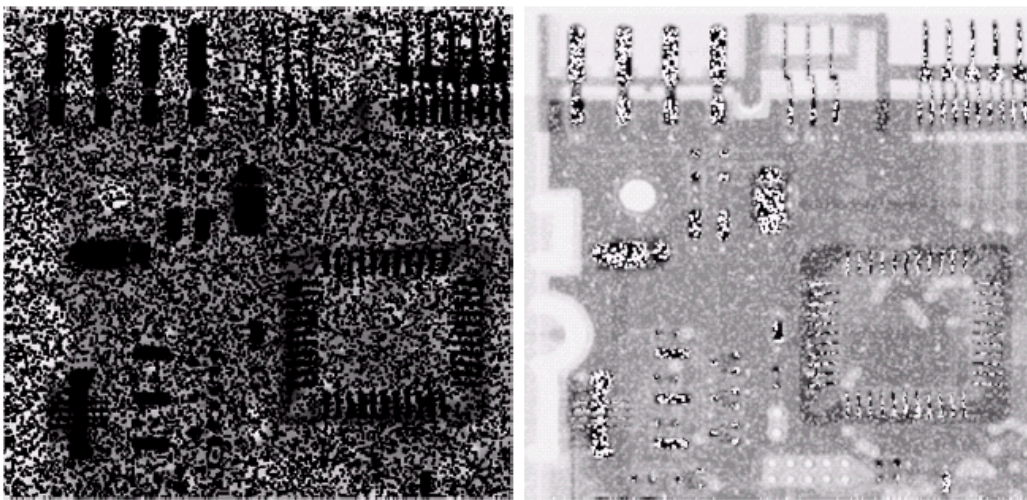
**FIGURE 5.7** (a) X-ray image.  
(b) Image corrupted by additive Gaussian noise. (c) Result of filtering with an arithmetic mean filter of size  $3 \times 3$ . (d) Result of filtering with a geometric mean filter of the same size. (Original image courtesy of Mr. Joseph E. Pascente, Lixi, Inc.)

a b  
c d

**FIGURE 5.8**

(a) Image corrupted by pepper noise with a probability of 0.1. (b) Image corrupted by salt noise with the same probability. (c) Result of filtering (a) with a  $3 \times 3$  contraharmonic filter of order 1.5. (d) Result of filtering (b) with  $Q = -1.5$ .





a b

**FIGURE 5.9** Results of selecting the wrong sign in contraharmonic filtering. (a) Result of filtering Fig. 5.8(a) with a contraharmonic filter of size  $3 \times 3$  and  $Q = -1.5$ . (b) Result of filtering 5.8(b) with  $Q = 1.5$ .

# Order-statistics filters

- Order-statistics filters: spatial filters whose response is based on ordering (ranking) the pixels in the subimage
- Median filters:

$$\hat{f}(x, y) = \underset{(s,t) \in S_{xy}}{\text{median}}\{g(s, t)\}$$

- Effective for salt and pepper noise

- Max and Min filters

$$\hat{f}(x, y) = \underset{(s,t) \in S_{xy}}{\max}\{g(s, t)\} \quad \hat{f}(x, y) = \underset{(s,t) \in S_{xy}}{\min}\{g(s, t)\}$$

- Max filter: useful for finding brightest points in an image (remove pepper noise)
- Min filter: useful for finding darkest points in an image (remove salt noise)

---

# Order-statistics filters

- Midpoint filter:

$$\hat{f}(x, y) = \frac{1}{2} \left[ \max_{(s,t) \in S_{xy}} \{g(s,t)\} + \min_{(s,t) \in S_{xy}} \{g(s,t)\} \right]$$

- Works best for Gaussian and uniform noise
- Alpha-trimmed mean filter
- $d/2$  lowest and  $d/2$  highest gray-levels are removed

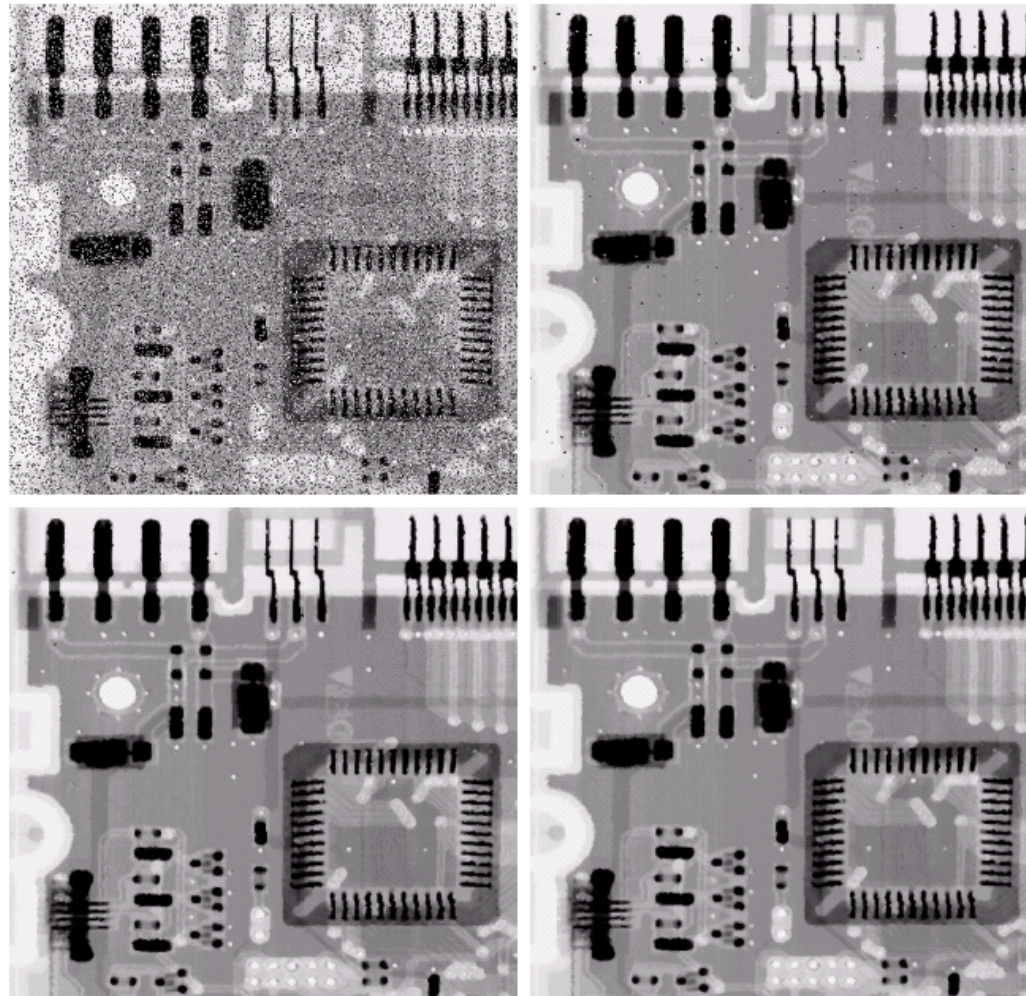
$$\hat{f}(x, y) = \frac{1}{mn - d} \sum_{(s,t) \in S_{xy}} g_r(s, t)$$

- Useful for combination of salt-pepper and Gaussian noise

a b  
c d

**FIGURE 5.10**

- (a) Image corrupted by salt-and-pepper noise with probabilities  $P_a = P_b = 0.1$ .  
(b) Result of one pass with a median filter of size  $3 \times 3$ .  
(c) Result of processing (b) with this filter.  
(d) Result of processing (c) with the same filter.



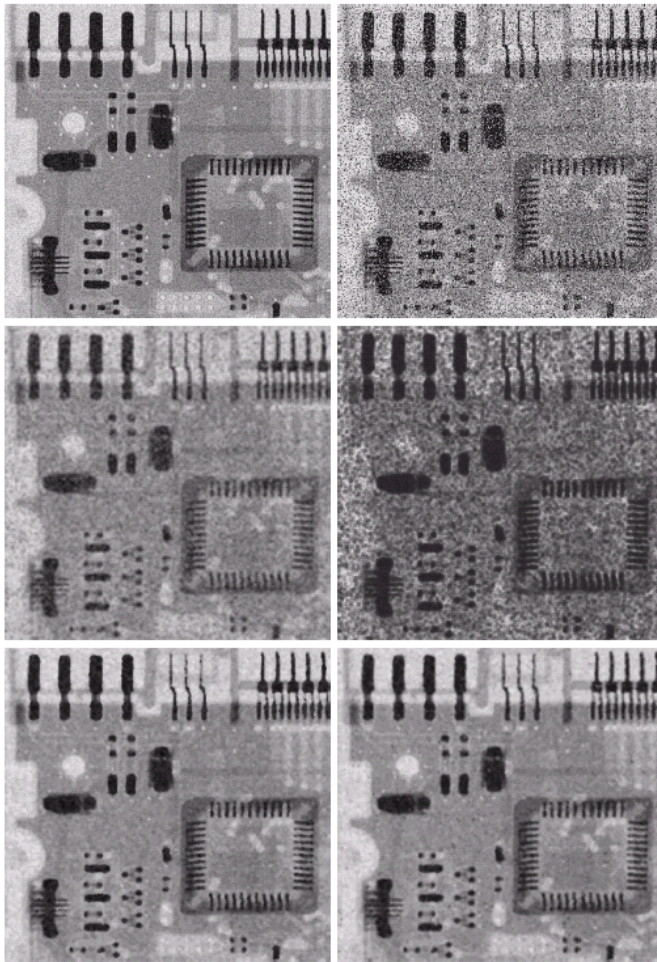


**FIGURE 5.12** (a) Image corrupted by additive uniform noise. (b) Image additionally corrupted by additive salt-and-pepper noise. Image in (b) filtered with a  $5 \times 5$ : (c) arithmetic mean filter; (d) geometric mean filter; (e) median filter; and (f) alpha-trimmed mean filter with  $d = 5$ .

---

# Adaptive filters

- Adaptive filters: behavior of the filter changes based on statistical characteristics of the image inside the subimage ( $S_{xy}$ )
- Adaptive filters have superior performance
- Price: increase in filter complexity

# Adaptive, local noise reduction filter

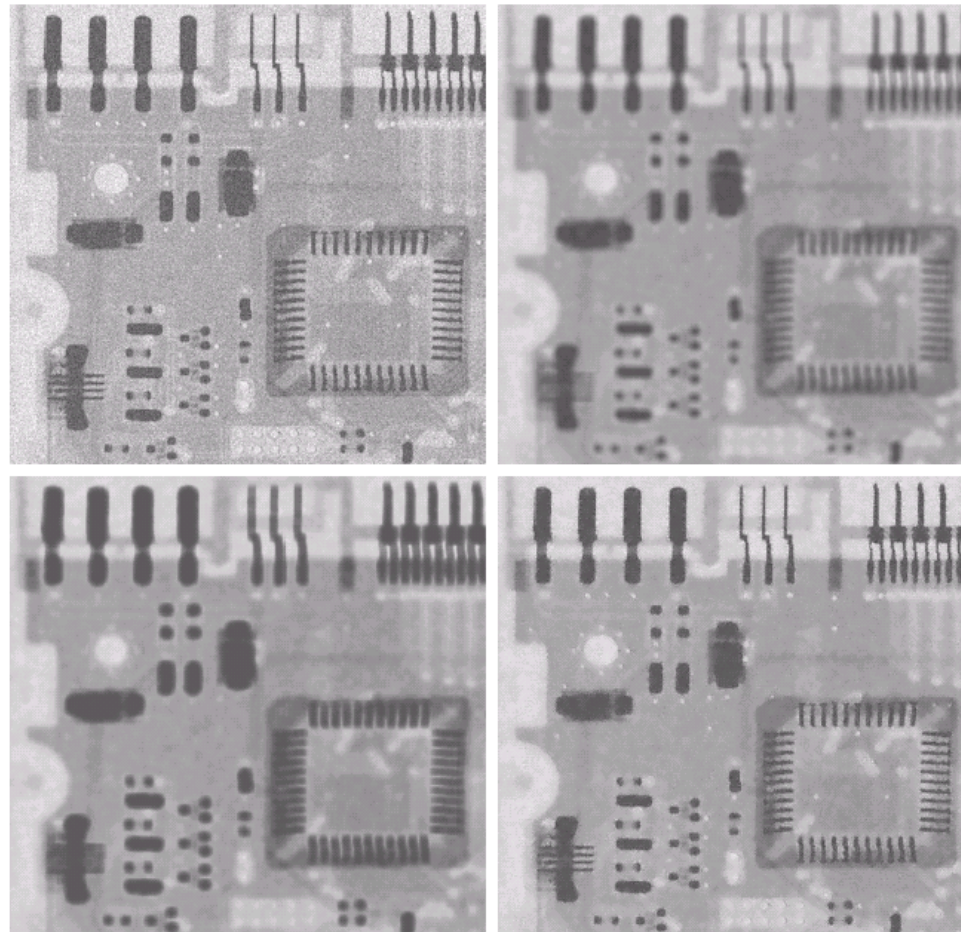
- Response of the filter is based on four quantities:
  1.  $g(x,y)$
  2.  $\sigma_{\eta}^2$  : variance of noise
  3.  $m_L$ : mean of pixels in  $S_{xy}$
  4.  $\sigma_L^2$ : variance of pixels in  $S_{xy}$
- The behavior of the filter:
  - If  $\sigma_{\eta}^2$  is zero, filter should return  $g(x,y)$
  - If  $\sigma_L^2$  is high (edges) the filter should return  $g(x,y)$
  - If the two variances are almost equal, the filter should return the mean of the pixels in  $S_{xy}$

$$\hat{f}(x, y) = g(x, y) - \frac{\sigma_{\eta}^2}{\sigma_L^2} [g(x, y) - m_L]$$

a b  
c d

**FIGURE 5.13**

- (a) Image corrupted by additive Gaussian noise of zero mean and variance 1000.  
(b) Result of arithmetic mean filtering.  
(c) Result of geometric mean filtering.  
(d) Result of adaptive noise reduction filtering. All filters were of size  $7 \times 7$ .



---

# Adaptive median filtering

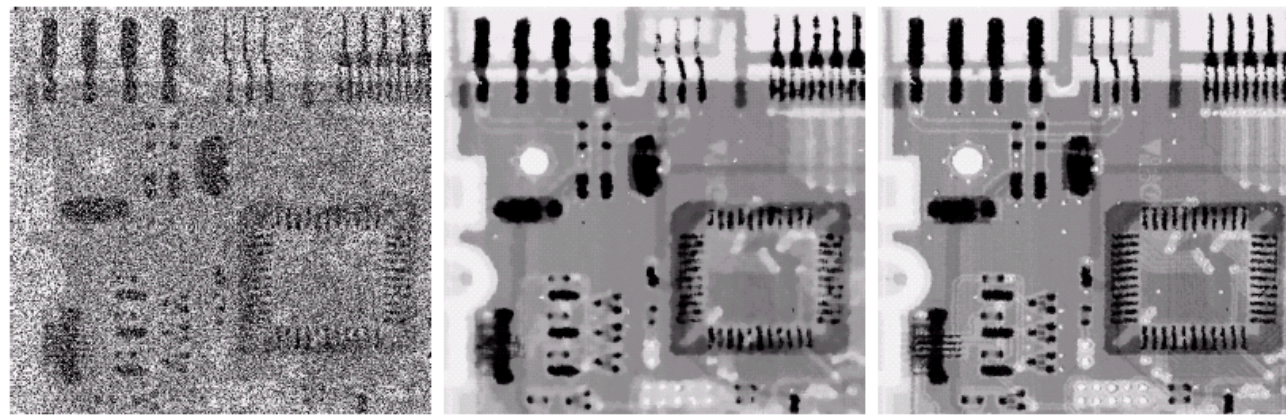
- Median filters perform well as long as the density of impulse noise is not large
- Adaptive median filter:
  - Handle dense impulse noise
  - Smoothes non-impulse noise
  - Preserves details
- $z_{\min}$ : minimum gray level in  $S_{xy}$
- $z_{\max}$ : maximum gray level in  $S_{xy}$
- $z_{\text{med}}$ : median gray level of  $S_{xy}$
- $z_{xy}$ : gray level at coordinate  $(x,y)$
- $S_{\max}$ : maximum allowed size of  $S_{xy}$

---

# Adaptive median filtering

- A
  - $A_1 = z_{\text{med}} - z_{\min}$
  - $A_2 = z_{\text{med}} - z_{\max}$
  - If  $A_1 > 0$  and  $A_2 < 0$  go to B else increase the window size
  - If window size  $< S_{\max}$  repeat A
  - Else output  $z_{xy}$
- B
  - $B_1 = z_{xy} - z_{\min}$
  - $B_2 = z_{xy} - z_{\max}$
  - If  $B_1 > 0$  and  $B_2 < 0$  output  $z_{xy}$
  - Else output  $z_{\text{med}}$

# Adaptive median filtering



a b c

**FIGURE 5.14** (a) Image corrupted by salt-and-pepper noise with probabilities  $P_a = P_b = 0.25$ . (b) Result of filtering with a  $7 \times 7$  median filter. (c) Result of adaptive median filtering with  $S_{\max} = 7$ .

---

# Periodic noise reduction

- Bandreject filters remove or attenuate a band of frequencies

$$H(u, v) = \begin{cases} 1 & D(u, v) < D_0 - \frac{W}{2} \\ 0 & D_0 - \frac{W}{2} \leq D(u, v) \leq D_0 + \frac{W}{2} \\ 1 & D(u, v) > D_0 + \frac{W}{2} \end{cases}$$

$$H(u, v) = \frac{1}{1 + \left[ \frac{D(u, v)W}{D^2(u, v) - D_0^2} \right]^{2n}}$$

$$H(u, v) = 1 - e^{-\frac{1}{2} \left[ \frac{D^2(u, v) - D_0^2}{D(u, v)W} \right]^2}$$

# Periodic noise reduction

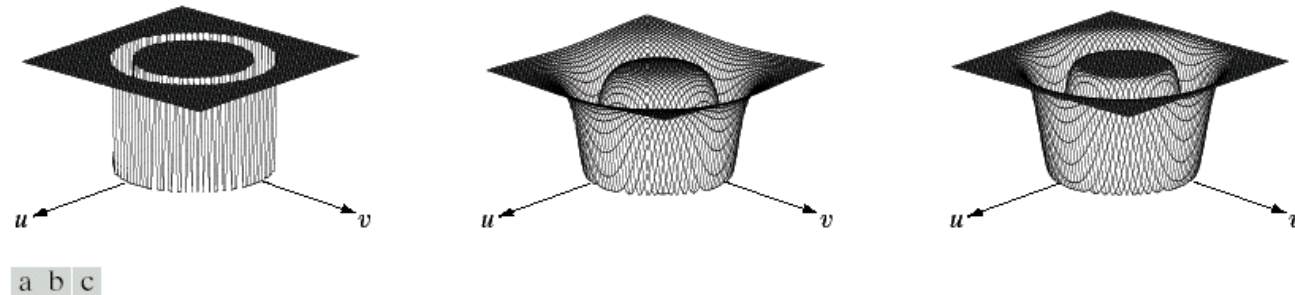
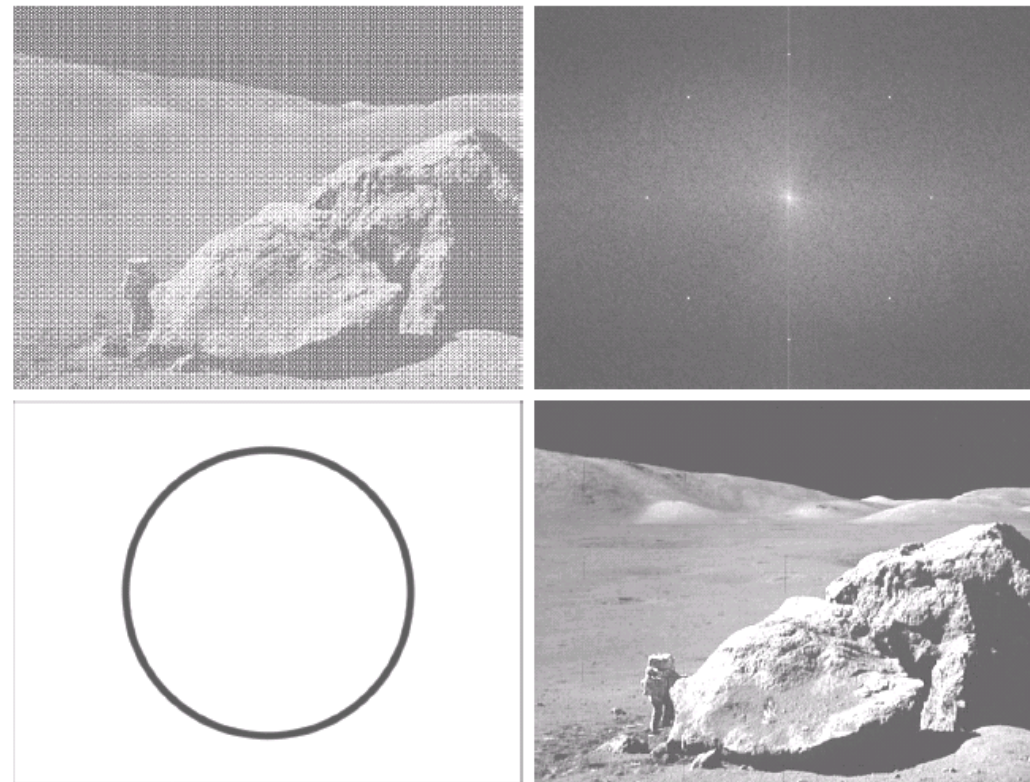


**FIGURE 5.15** From left to right, perspective plots of ideal, Butterworth (of order 1), and Gaussian bandreject filters.

# Periodic noise reduction



a b  
c d

**FIGURE 5.16**  
(a) Image corrupted by sinusoidal noise.  
(b) Spectrum of (a).  
(c) Butterworth bandreject filter (white represents 1).  
(d) Result of filtering. (Original image courtesy of NASA.)

---

# Periodic noise reduction

- A bandpass filter performs the opposite of a bandreject filter.
  - $H_{bp}(u,v) = 1 - H_{br}(u,v)$
- A notch filter rejects (or passes) frequencies in predefined neighborhood about a center frequency
- Due to symmetry of the FT, notch filters must appear in symmetric pairs about the origin in order to obtain meaningful results

---

# Periodic noise reduction

$$H(u, v) = \begin{cases} 0 & D_1(u, v) \leq D_0, D_2(u, v) \leq D_0 \\ 1 & \text{otherwise} \end{cases}$$

$$H(u, v) = \frac{1}{1 + \left[ \frac{D_0}{D_1(u, v)D_2(u, v)} \right]^n}$$

$$H(u, v) = 1 - e^{-\frac{1}{2} \left[ \frac{D_1(u, v)D_2(u, v)}{D_0^2} \right]}$$

$$D_1(u, v) = (u - u_0)^2 + (v - v_0)^2$$

$$D_2(u, v) = (u + u_0)^2 + (v + v_0)^2$$

# Periodic noise reduction

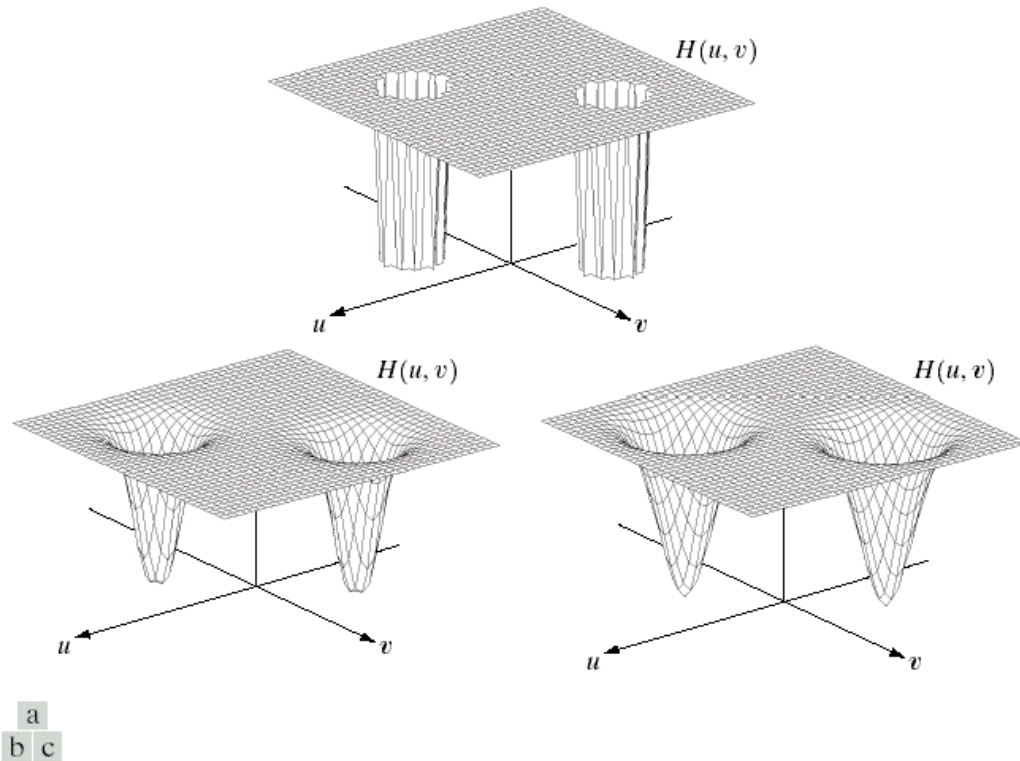
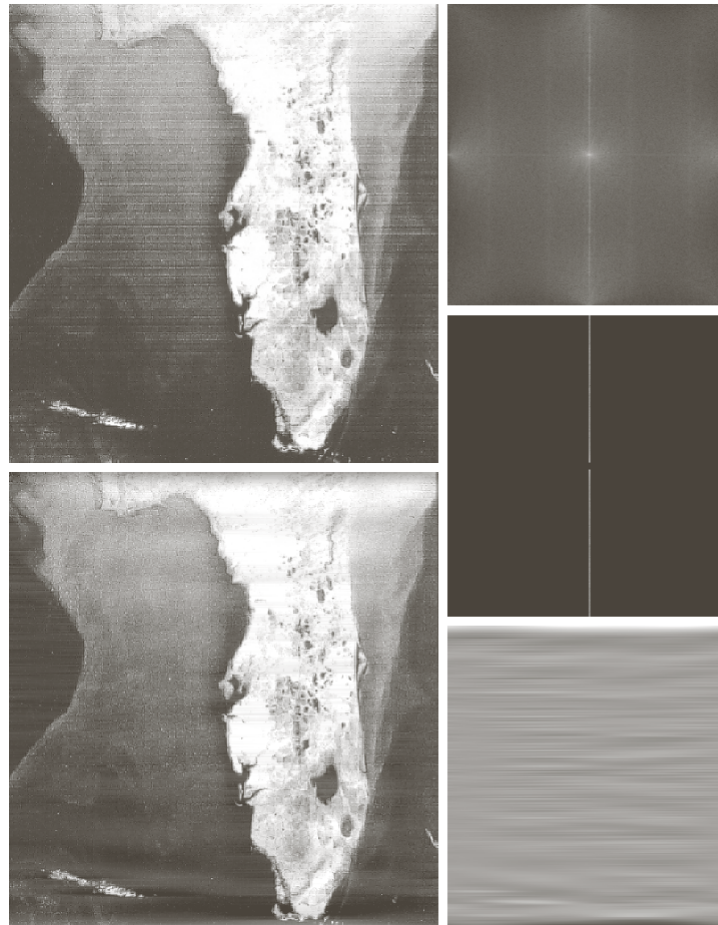


**FIGURE 5.18** Perspective plots of (a) ideal, (b) Butterworth (of order 2), and (c) Gaussian notch (reject) filters.



a b  
c d  
e

**FIGURE 5.19**  
(a) Satellite image of Florida and the Gulf of Mexico showing horizontal scan lines.  
(b) Spectrum. (c) Notch pass filter superimposed on (b). (d) Spatial noise pattern.  
(e) Result of notch reject filtering.  
(Original image courtesy of NOAA.)

# Estimation of degradation

- Since degradations are modeled as being the result of convolution, restoration is sometimes called deconvolution.
- Estimation of the degradation function:
  1. Observation
  2. Experimentation
  3. Mathematical modeling

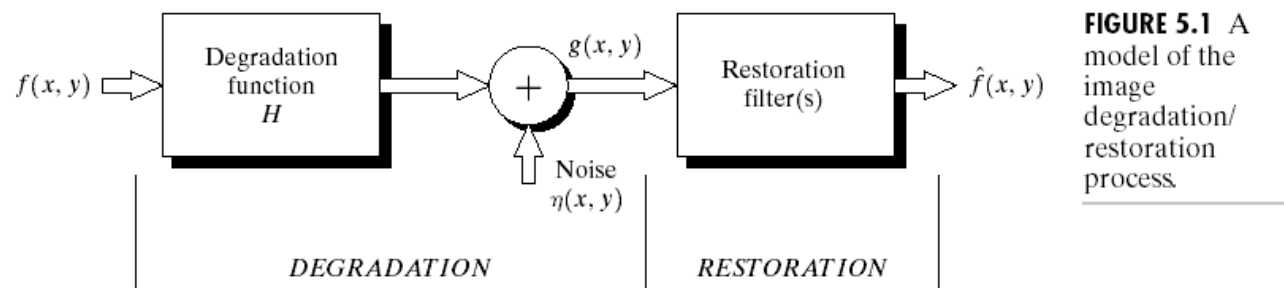


**FIGURE 5.1** A model of the image degradation/ restoration process.

---

## Estimation by image observation

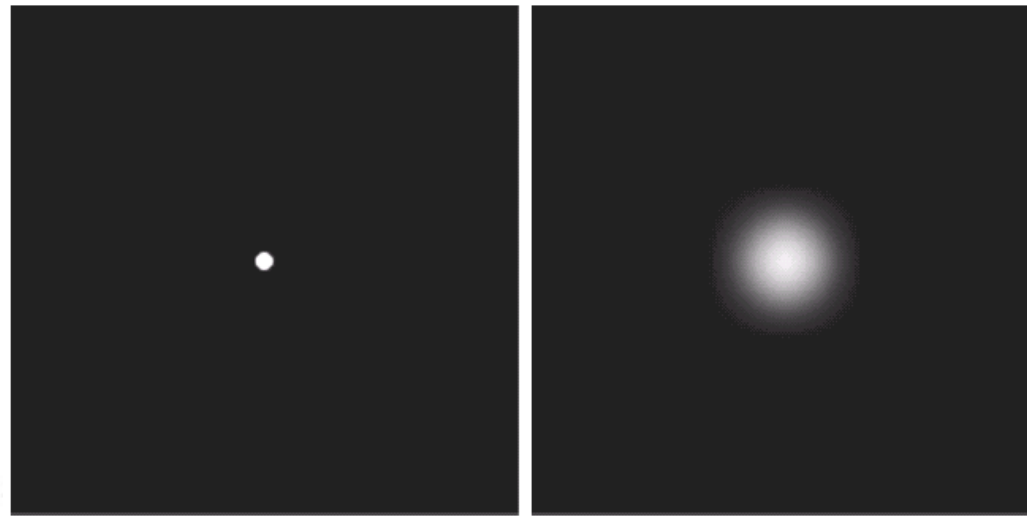
- We are given a degraded image without any knowledge of  $H$ .
- We look at a small section of the image containing simple structures (e.g., part of an object and the background)
- Using sample gray levels of the object and background, we can construct an unblurred image of the subimage  $\hat{f}_s(x, y)$

$$H_s(u, v) = \frac{\hat{G}_s(u, v)}{\hat{F}_s(u, v)}$$

# Estimation by Experimentation

- If equipment similar to the equipment used to acquire the degraded image is available it is possible to obtain an accurate estimate of the degradation.
- The idea is to obtain the impulse response of the degradation by imaging an impulse (small dot of light) using the system

$$H(u, v) = \frac{G(u, v)}{A}$$



a b

**FIGURE 5.24**  
Degradation  
estimation by  
impulse  
characterization.  
(a) An impulse of  
light (shown  
magnified).  
(b) Imaged  
(degraded)  
impulse.

# Estimation by modeling

- Approach: derive a mathematical model starting from basic principles
- Example: Images blurred by motion

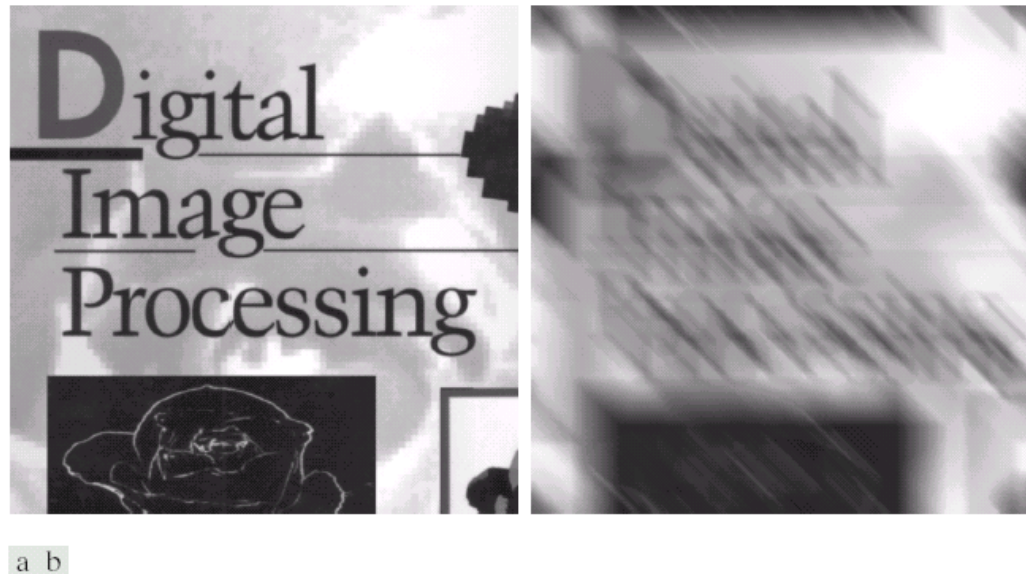


**FIGURE 5.26** (a) Original image. (b) Result of blurring using the function in Eq. (5.6-11) with  $a = b = 0.1$  and  $T = 1$ .

a b  
c d

**FIGURE 5.25**

Illustration of the atmospheric turbulence model.  
(a) Negligible turbulence.  
(b) Severe turbulence,  
 $k = 0.0025$ .  
(c) Mild turbulence,  
 $k = 0.001$ .  
(d) Low turbulence,  
 $k = 0.00025$ .  
(Original image courtesy of NASA.)



# Inverse filtering

a b  
c d

**FIGURE 5.27**

Restoring

Fig. 5.25(b) with  
Eq. (5.7-1).

(a) Result of  
using the full  
filter. (b) Result  
with  $H$  cut off  
outside a radius of  
40; (c) outside a  
radius of 70; and  
(d) outside a  
radius of 85.



# Wiener filtering



**FIGURE 5.28** Comparison of inverse- and Wiener filtering. (a) Result of full inverse filtering of Fig. 5.25(b). (b) Radially limited inverse filter result. (c) Wiener filter result.

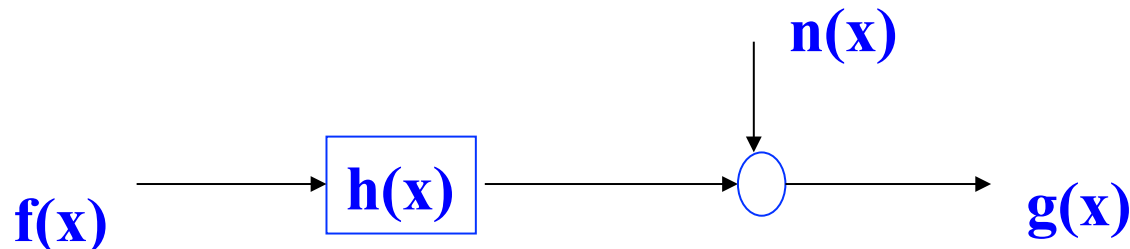
# Wiener filtering



FIGURE 5.29 (a) Image corrupted by motion blur and additive noise. (b) Result of inverse filtering. (c) Result of Wiener filtering. (d)–(f) Same sequence, but with noise variance one order of magnitude less. (g)–(i) Same sequence, but noise variance reduced by five orders of magnitude from (a). Note in (h) how the deblurred image is quite visible through a “curtain” of noise.

# A Simple Example

- 1-D signal
- $h$  is a 2 point signal ( $h(0)$  and  $h(1)$ )
- $f$  is also a 2 point signal
- $g$  is observed: find  $f(0)$  and  $f(1)$  from  $g(0)$ ,  $g(1)$ ,  $g(2)$



---

# A Simple Example

$$g(x) = h(x) * f(x) + n(x)$$

$$g(x) = \sum_{x'=0}^1 f(x-x')h(x') + n(x)$$

$$g(0) = f(0)h(0) + f(-1)h(1) + n(0)$$

$$g(1) = f(1)h(0) + f(0)h(1) + n(1)$$

$$g(2) = f(2)h(0) + f(1)h(1) + n(2)$$

$$g(0) = f(0)h(0) + n(0)$$

$$g(1) = f(1)h(0) + f(0)h(1) + n(1)$$

$$g(2) = f(1)h(1) + n(2)$$

---

# A Simple Example

- If the noise is not ignored, we have five unknowns and only three equations.
- The original signal ( $f$ ) cannot be determined uniquely.
- This is an example of an **ill-conditioned** problem.
- Some other knowledge about  $f$  is necessary.

$$g(0) = f(0)h(0) + n(0)$$

$$g(1) = f(1)h(0) + f(0)h(1) + n(1)$$

$$g(2) = f(1)h(1) + n(2)$$

$$\min \{[f(0) - f(1)]^2\}$$

---

# Constrained Least Square Filtering

- $\mathbf{g} = \mathbf{H}\mathbf{f} + \mathbf{n}$
- Find a restoration filter such that the output of the filter is smooth:

$$C = \sum_{x=0}^{M-1} \sum_{y=0}^{N-1} [\nabla^2 \hat{f}(x, y)]^2$$

$$\nabla^2 \hat{f}(x, y) \approx 4\hat{f}(x, y) - \hat{f}(x+1, y) - \hat{f}(x-1, y) - \hat{f}(x, y+1) - \hat{f}(x, y-1)$$

$$\left\| \mathbf{g} - H \hat{\mathbf{f}} \right\|^2 = \|\mathbf{n}\|^2$$

- After a lengthy procedure (which has been removed in the new edition of the book) using the fact that the matrix  $\mathbf{H}$  is circular it can be shown that:

---

# Constrained Least Square Filtering

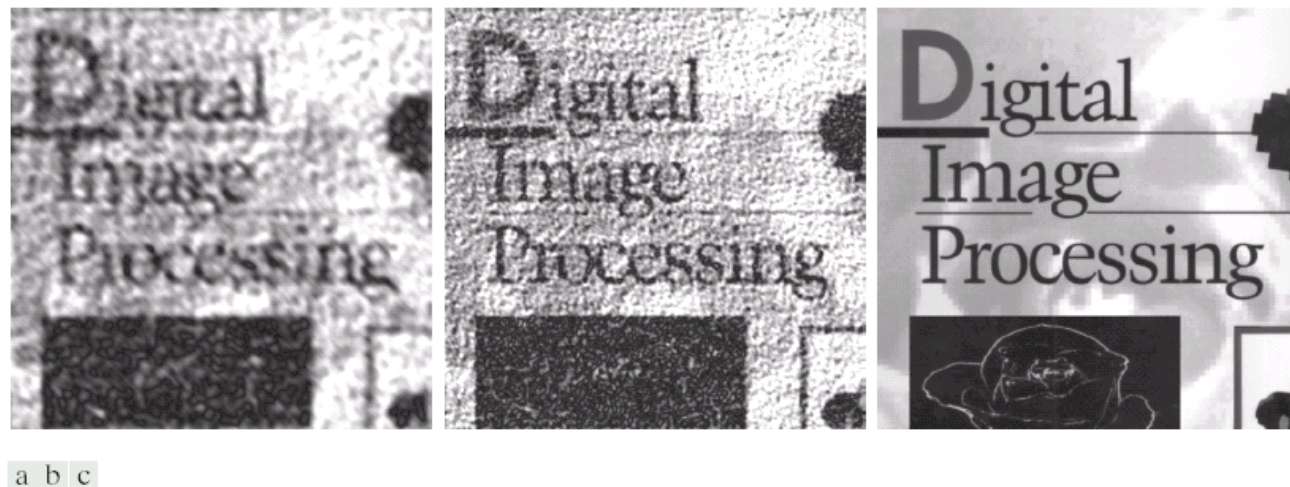
$$M(u, v) = \frac{H^*(u, v)}{|H(u, v)|^2 + \gamma |P(u, v)|^2}$$

- $P(u, v)$  is the Fourier transform of the Laplacian operator:

$$p(x, y) = \begin{bmatrix} 0 & -1 & 0 \\ -1 & 4 & -1 \\ 0 & -1 & 0 \end{bmatrix}$$

- $\gamma$  is a parameter.
- $p(x, y)$  should be padded to a proper size.
- Although mathematical method exists for finding  $\gamma$ , in most practical cases  $\gamma$  is selected by trial and error.

# Constrained Least Square Filtering



a b c

**FIGURE 5.30** Results of constrained least squares filtering. Compare (a), (b), and (c) with the Wiener filtering results in Figs. 5.29(c), (f), and (i), respectively.

---

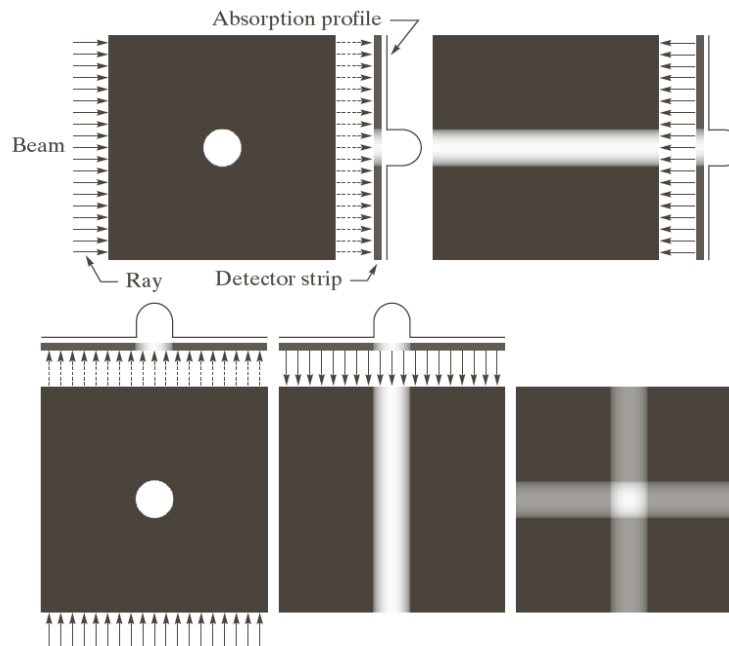
# Geometric Mean Filter

- Generalization of Wiener filter:

$$M(u, v) = \left[ \frac{H^*(u, v)}{|H(u, v)|^2} \right]^\alpha \left[ \frac{H^*(u, v)}{|H(u, v)|^2 + \beta \left[ \frac{S_n(u, v)}{S_f(u, v)} \right]} \right]^{1-\alpha}$$

- $\alpha$  and  $\beta$  : positive real constants
- $\alpha=1$  : inverse filter
- $\alpha=0$  : parametric Wiener filter
- $\alpha=0, \beta=1$  : Wiener filter
- $\alpha=1/2, \beta=1$  : spectrum equalization filter

# Image Reconstruction from Projections



a b  
c d e

**FIGURE 5.32**  
(a) Flat region showing a simple object, an input parallel beam, and a detector strip.  
(b) Result of back-projecting the sensed strip data (i.e., the 1-D absorption profile).  
(c) The beam and detectors rotated by 90°.  
(d) Back-projection.  
(e) The sum of (b) and (d). The intensity where the back-projections intersect is twice the intensity of the individual back-projections.

# Image Reconstruction from Projections

a	b	c
d	e	f

**FIGURE 5.33**

(a) Same as Fig.  
5.32(a).

(b)–(e)  
Reconstruction  
using 1, 2, 3, and 4  
backprojections  $45^\circ$   
apart.

(f) Reconstruction  
with 32 backprojec-  
tions  $5.625^\circ$  apart  
(note the blurring).

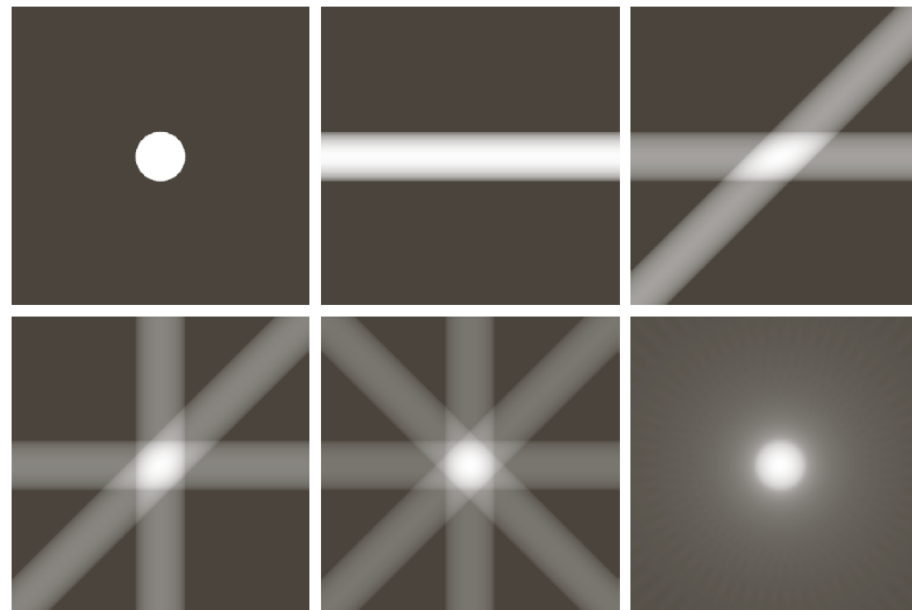


# Image Reconstruction from Projections

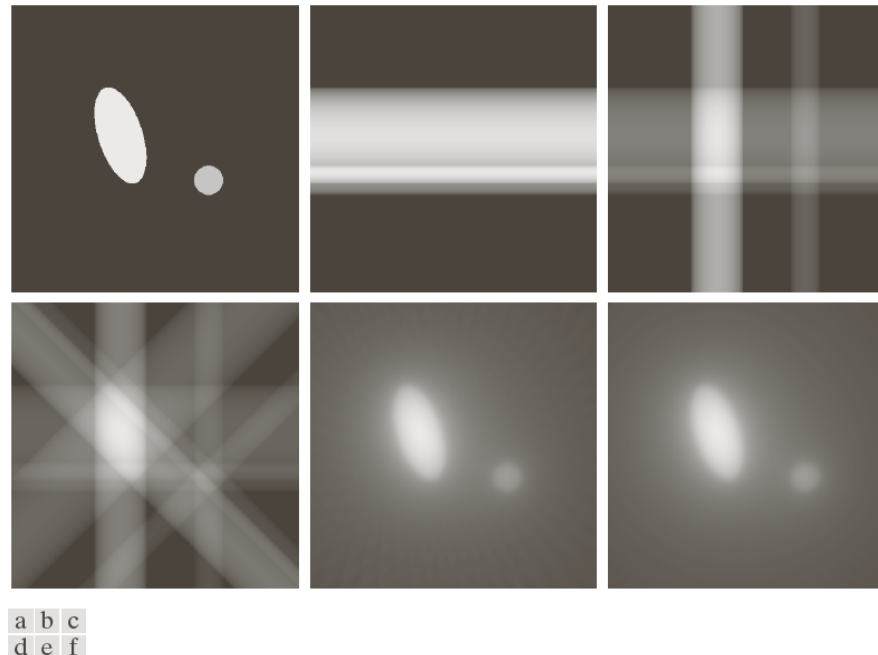


**FIGURE 5.34** (a) A region with two objects. (b)–(d) Reconstruction using 1, 2, and 4 backprojections  $45^\circ$  apart. (e) Reconstruction with 32 backprojections  $5.625^\circ$  apart. (f) Reconstruction with 64 backprojections  $2.8125^\circ$  apart.

---

# Image Reconstruction from Projections

- First generation (G1) scanners: pencil x-ray beam, a single detector
  - For a given angle of rotation, source/detector pair is translated
- Second generation (G2): the beam is fan shaped
- Third generation (G3): a bank of detector long enough to cover the entire field of view of a wide beam
- Fourth generation (G4): a circular ring of detectors, source rotates
- Fifth generation (G5) also known as electron beam computed tomography (EBTC): eliminates all mechanical motion, the beam is controlled electromagnetically

---

# Image Reconstruction from Projections

- Conventional way of generating CT image: keep patient stationary during scanning, halt scan, increment position of the patient, obtain the next image
- Long procedure
- Six generation (helical CT): a G3 or G4 scanner is configured using slip rings that eliminates need for cables
  - Source/detector pair move along the axis perpendicular to the scan
- Seventh generation (G7) scanners: a thick fan beam and banks of detectors are used to collect data of cross sectional slabs
  - Lower cost and dosage

# Image Reconstruction from Projections

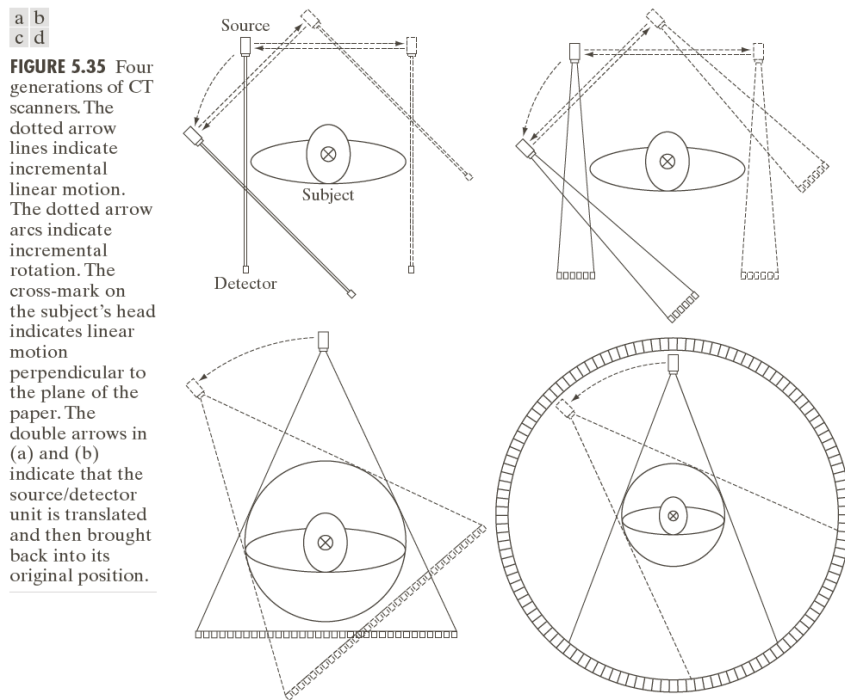


**FIGURE 5.35** Four generations of CT scanners. The dotted arrow lines indicate incremental linear motion. The dotted arrow arcs indicate incremental rotation. The cross-mark on the subject's head indicates linear motion perpendicular to the plane of the paper. The double arrows in (a) and (b) indicate that the source/detector unit is translated and then brought back into its original position.

# Image Reconstruction from Projections

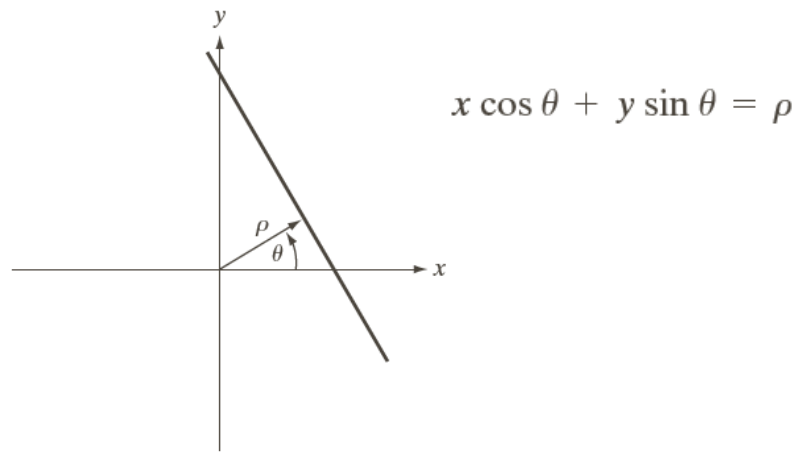


**FIGURE 5.36** Normal representation of a straight line.

# Image Reconstruction from Projections

**FIGURE 5.37**  
Geometry of a  
parallel-ray beam.

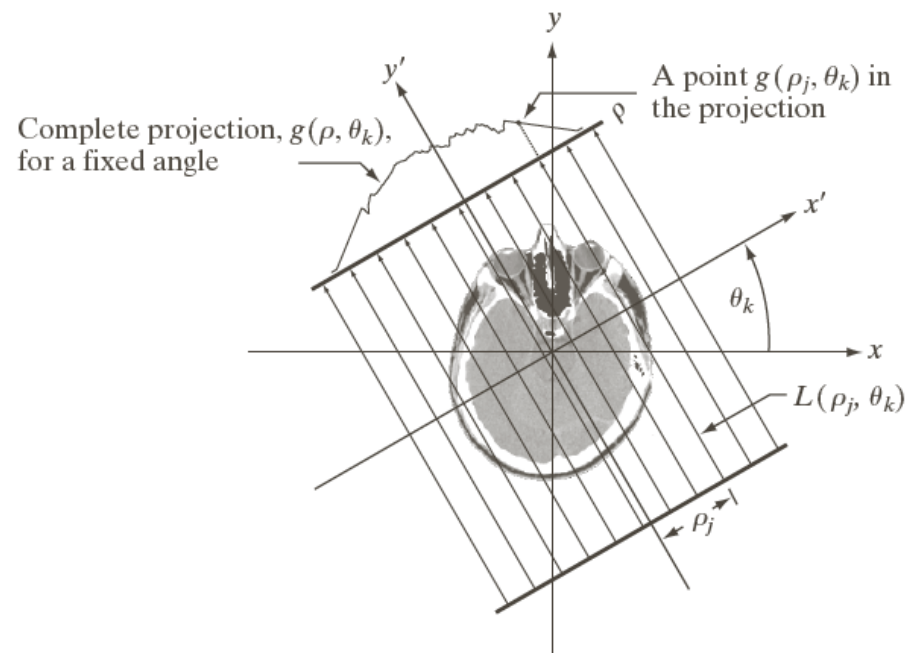


# Image Reconstruction from Projections

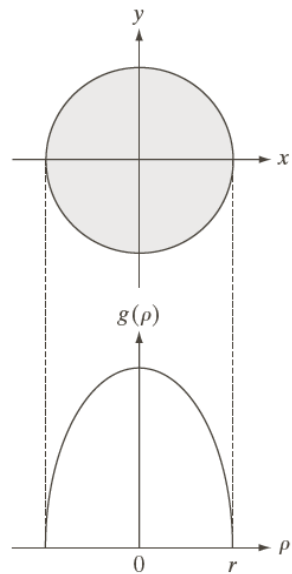


**FIGURE 5.38** A disk and a plot of its Radon transform, derived analytically. Here we were able to plot the transform because it depends only on one variable. When  $g$  depends on both  $\rho$  and  $\theta$ , the Radon transform becomes an image whose axes are  $\rho$  and  $\theta$ , and the intensity of a pixel is proportional to the value of  $g$  at the location of that pixel.

# Image Reconstruction from Projections

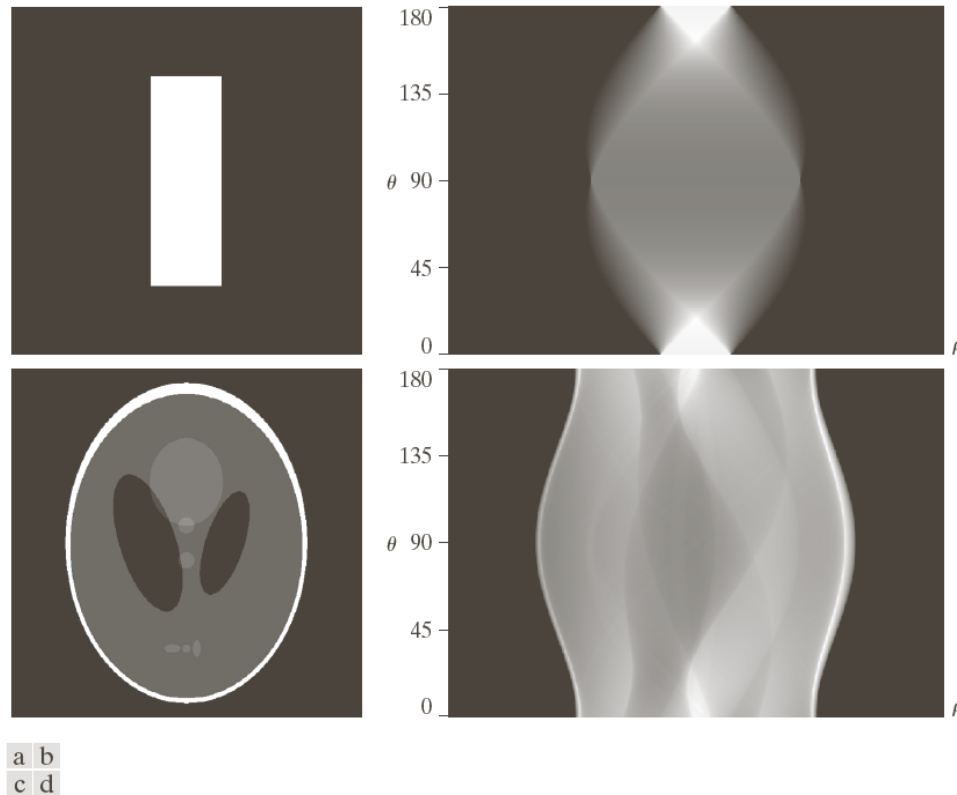
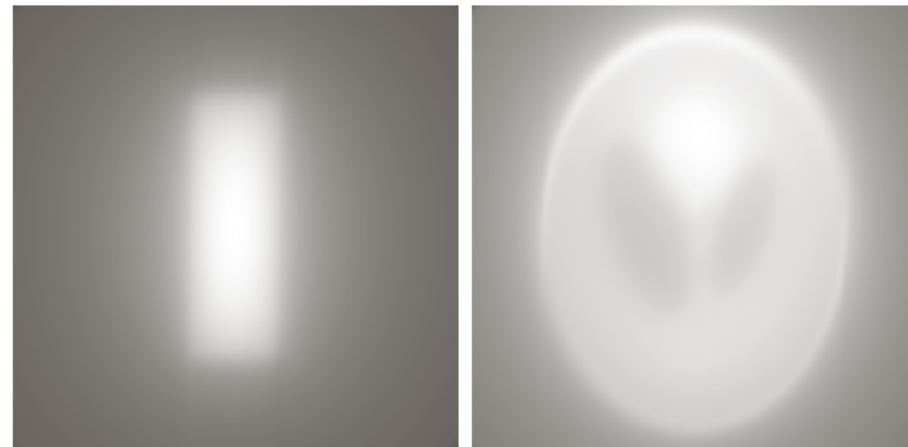


**FIGURE 5.39** Two images and their sinograms (Radon transforms). Each row of a sinogram is a projection along the corresponding angle on the vertical axis. Image (c) is called the *Shepp-Logan phantom*. In its original form, the contrast of the phantom is quite low. It is shown enhanced here to facilitate viewing.

---

# Image Reconstruction from Projections



a b

**FIGURE 5.40**  
Backprojections  
of the sinograms  
in Fig. 5.39.

---

# Image Reconstruction from Projections

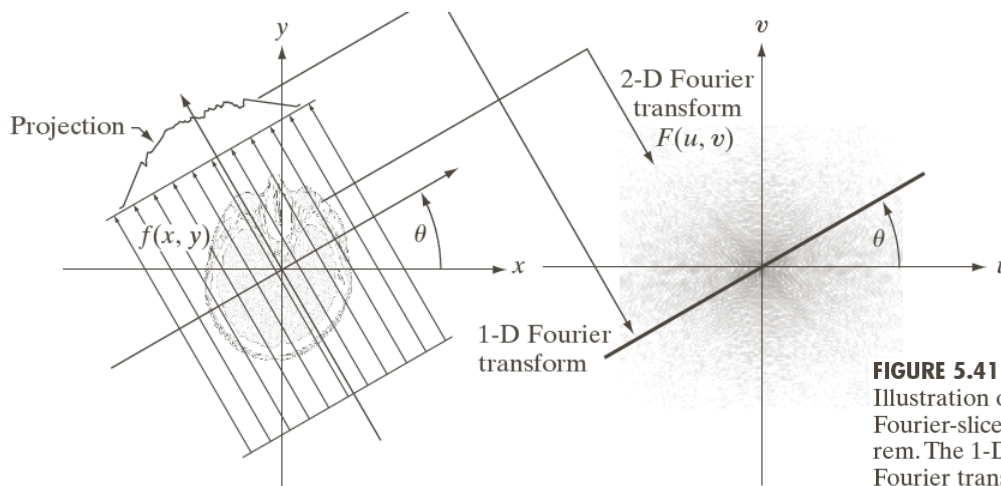
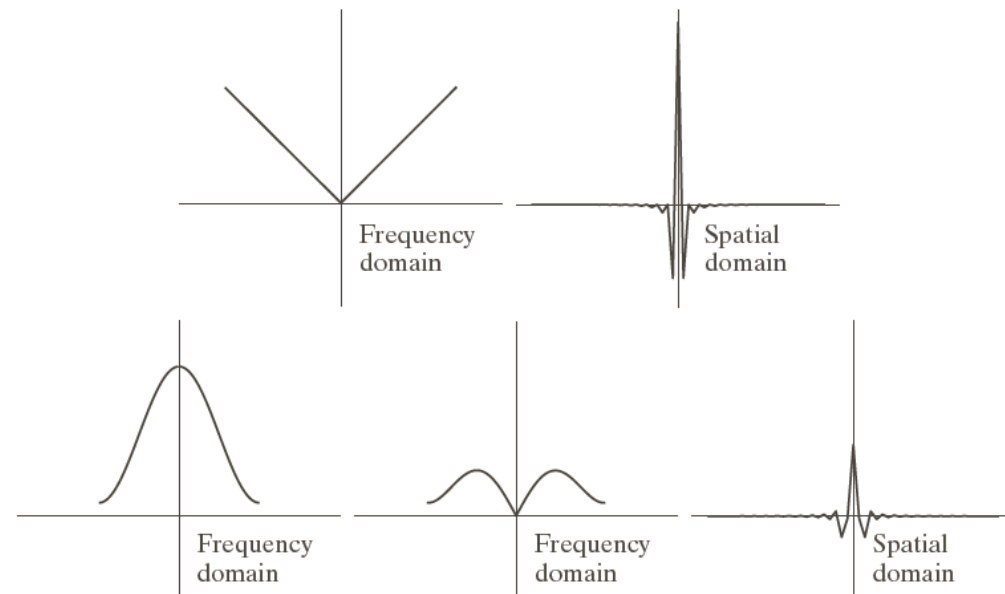


**FIGURE 5.41**  
Illustration of the Fourier-slice theorem. The 1-D Fourier transform of a projection is a slice of the 2-D Fourier transform of the region from which the projection was obtained. Note the correspondence of the angle  $\theta$ .

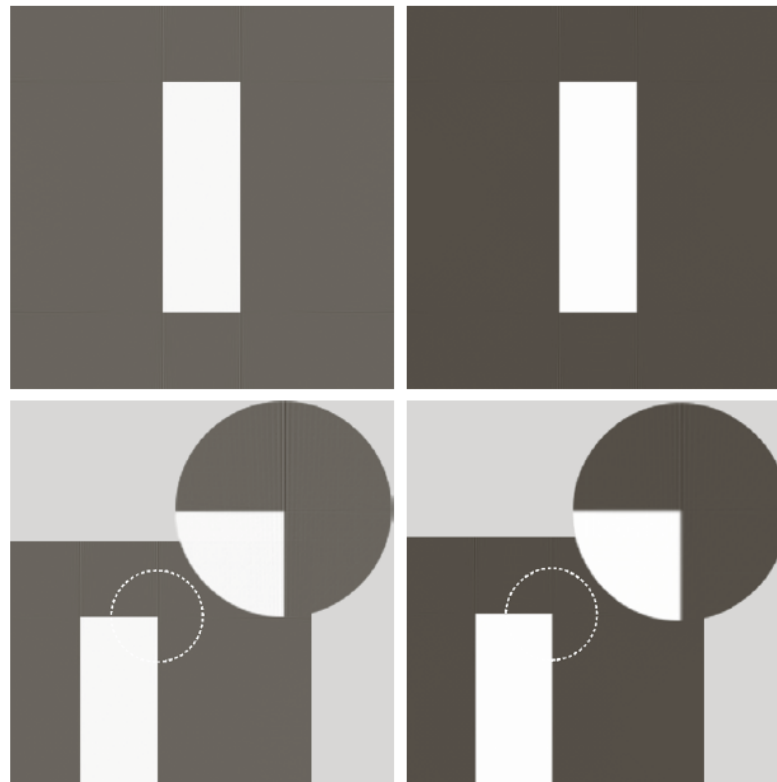
# Image Reconstruction from Projections



a b  
c d e

**FIGURE 5.42**  
(a) Frequency domain plot of the filter  $|\omega|$  after band-limiting it with a box filter. (b) Spatial domain representation.  
(c) Hamming windowing function.  
(d) Windowed ramp filter, formed as the product of (a) and (c). (e) Spatial representation of the product (note the decrease in ringing).

# Image Reconstruction from Projections



a b  
c d

**FIGURE 5.43**  
Filtered back-projections of the rectangle using (a) a ramp filter, and (b) a Hamming-windowed ramp filter. The second row shows zoomed details of the images in the first row. Compare with Fig. 5.40(a).

# Image Reconstruction from Projections



a b

**FIGURE 5.44**  
Filtered  
backprojections of  
the head phantom  
using (a) a ramp  
filter; and (b)  
a Hamming-windowed  
ramp filter. Compare  
with Fig. 5.40(b).

# Image Reconstruction from Projections

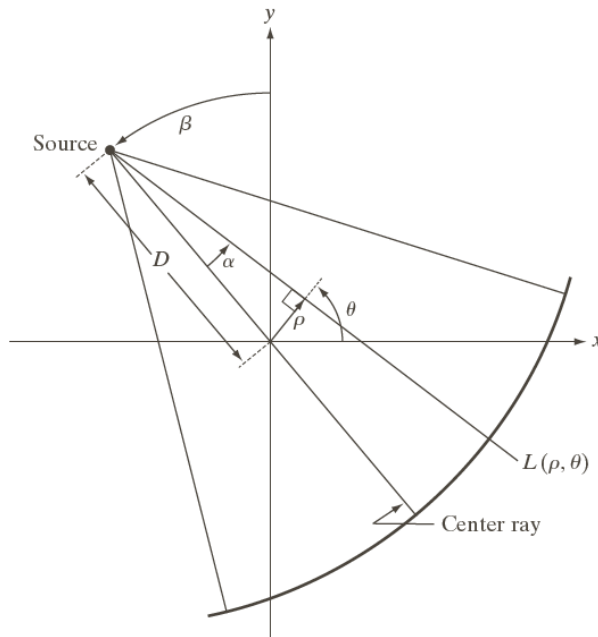


**FIGURE 5.45**  
Basic fan-beam geometry. The line passing through the center of the source and the origin (assumed here to be the center of rotation of the source) is called the *center ray*.

# Image Reconstruction from Projections

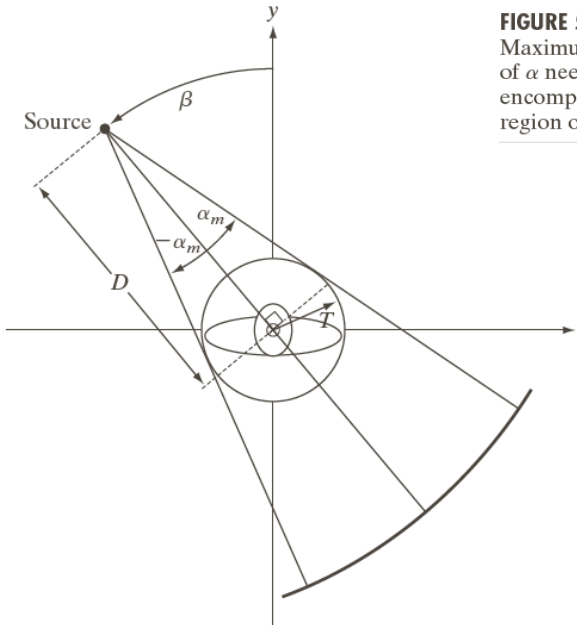


**FIGURE 5.46**  
Maximum value  
of  $\alpha$  needed to  
encompass a  
region of interest.

# Image Reconstruction from Projections

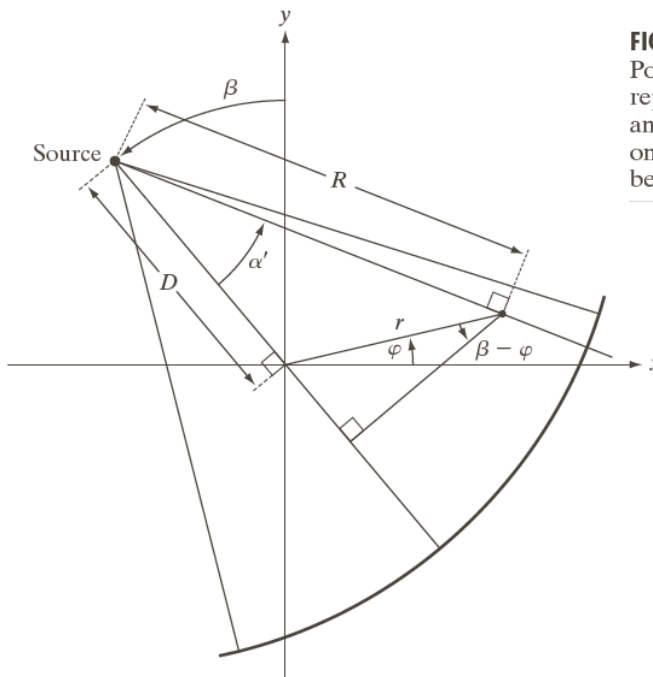
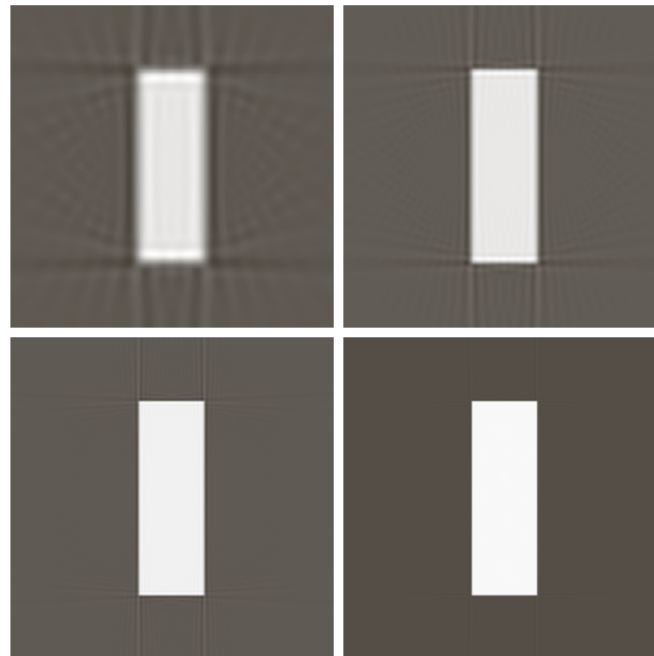


**FIGURE 5.47**  
Polar  
representation of  
an arbitrary point  
on a ray of a fan  
beam.

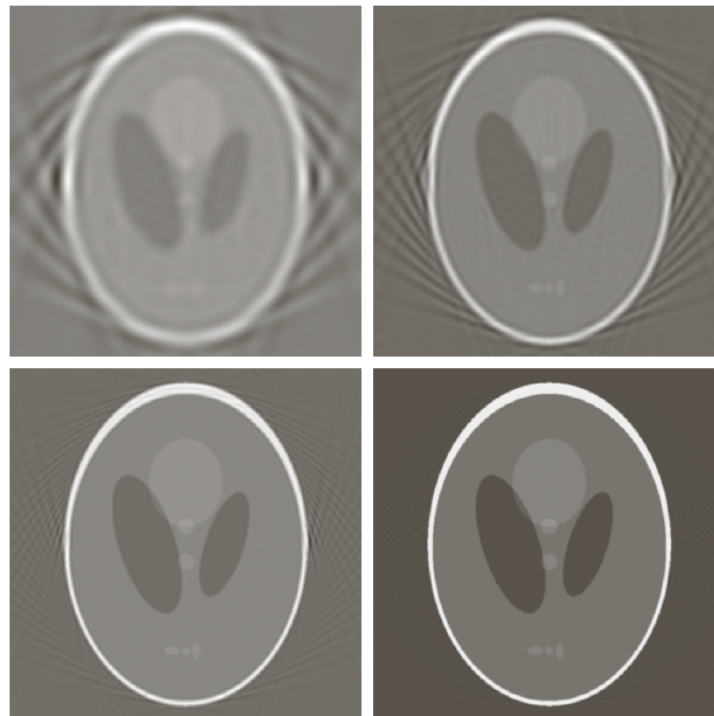
# Image Reconstruction from Projections



a b  
c d

**FIGURE 5.48**  
Reconstruction of  
the rectangle  
image from  
filtered fan  
backprojections.  
(a)  $1^\circ$  increments  
of  $\alpha$  and  $\beta$ .  
(b)  $0.5^\circ$   
increments.  
(c)  $0.25^\circ$   
increments.  
(d)  $0.125^\circ$   
increments.  
Compare (d) with  
Fig. 5.43(b).

# Image Reconstruction from Projections



a b  
c d

**FIGURE 5.49**  
Reconstruction of  
the head phantom  
image from  
filtered fan  
backprojections.  
(a)  $1^\circ$  increments  
of  $\alpha$  and  $\beta$ .  
(b)  $0.5^\circ$   
increments.  
(c)  $0.25^\circ$   
increments.  
(d)  $0.125^\circ$   
increments.  
Compare (d) with  
Fig. 5.44(b).